

## DETECTING KEY SOURCES OF UNCERTAINTY IN PROJECTIONS RELATED TO HEDGING RULE-BASED RESERVOIR OPERATIONS

Umut OKKAN<sup>1</sup>, Zeynep Beril ERSOY<sup>1</sup>, Okan FİSTİKOGLU<sup>2</sup>

<sup>1</sup>Department of Civil Engineering, Hydraulic Division, Balikesir University, Cagis Campus, Balikesir, Türkiye *E-mail: umutokkan@balikesir.edu.tr, zeynepberil.ersoy@balikesir.edu.tr*

<sup>2</sup>Department of Civil Engineering, Hydraulic Division, Dokuz Eylul University, Tinaztepe Campus, Izmir, Türkiye *E-mail : okan.fistikoglu@deu.edu.tr*

**Abstract.** Dam reservoirs designed on past hydrological records exhibit increasing vulnerability and uncertainty propagating over time under changing runoff regimes triggered by climate change. In particular, standard operating policy (SOP), which focuses on directly meeting target demand and does not include any operators to mitigate future shortage risks, becomes sensitive to variability in projected inflows, leading to sudden and severe vulnerabilities in dry seasons. In this study, the uncertainties in projected system vulnerability (VUL) for the Tahtali reservoir in western Turkey were analyzed under a total of 140 streamflow projections obtained from a combination of five global climate models (GCMs), two emission scenarios (ESs), two downscaling methods, and 7 hydrological models (HMs). In this context, a two-dimensional hedging model (HDG-2d) and SOP reservoir operation models were examined over the 2021–2099 projection horizon. Four-factor analysis of variance (four-way ANOVA) showed that 36% of the total VUL variance under SOP was due to the HM selection, and interaction terms made a significant contribution to the total uncertainty. Compared to the SOP, the HDG-2d model significantly attenuated the variability in VUL caused by the HM selection, reducing the total uncertainty by 65%. More importantly, this model ensured that 86% of the 140 projection variants remained below the threshold value of 0.25. On the other hand, the GCM and ES variance contributions to the total projection variance under HDG-2d increased to 20% and 42%, respectively. Rising temperature and evaporation signals, particularly in the pessimistic RCP8.5 scenario, led to the parameterization of more restrictive release strategies. Therefore, the fact that emission scenario selection becomes more temporally influential in projections on temperature and evaporation rather than annual mean inflow changes reveals the response of HDG-2d to these varying climate signals. Yet, it would still be inappropriate to praise the higher VUL values obtained under SOP despite its relatively lower uncertainty in certain sources. Interestingly, the HDG-2d model can be an important tool for decision-makers because of its ability to suppress HM-induced low-flow volatility and its adaptive structure that can account for GCM-driven hydro-meteorological changes.

**Keywords:** Reservoir operation, adaptive hedging rule, uncertainty, system vulnerability.

### 1 INTRODUCTION

Downscaling studies conducted in basins within the Mediterranean climate zone, including Türkiye, where global climate models (GCMs) are operated under Representative Concentration Pathways (RCP) scenarios, have projected that temperatures are expected to increase in the future, while precipitation and runoff patterns are likely to decrease, albeit with notable uncertainties

(Bozkurt et al., 2015; Okkan et al., 2024). These climate change-induced impacts are reflected in the hydrological process and consequently affect dam reservoirs, which are the most critical infrastructure for the development and management of integrated water resources. Both climatic factors and the increasing demand for water use due to population growth and urbanization are increasingly challenging decision-makers and management institutions in the context of balanced water allocation. Therefore, forward-looking studies are necessary to mitigate the potential impacts of climate change in the future and ensure the sustainability of reservoir releases.

Although GCMs employed by researchers can provide long-term projections, the fact that the modeling process carries significant uncertainties poses another issue. Previous studies indicate that uncertainties in climate change projections can arise from various sources, but the main factors that stand out are model-based uncertainties and those from emission scenarios (Yip et al., 2011). Model uncertainties stem from a lack of complete understanding of the relevant physical process and implementation constraints, while the internal variability also affects the projection spread (Hawkins and Sutton, 2009, 2011; Yip et al., 2011; Orlowsky and Seneviratne, 2013). All these studies, which evaluate distinct uncertainty components, mostly focus on variables such as precipitation, temperature and runoff, whereas there are a scant number of papers that address uncertainty in projected reservoir operation outputs (e.g., Okkan et al., 2023).

It has been emphasized that when examining sources of uncertainty in climate projections, using multi-model ensembles rather than a single GCM is more essential (Knutti et al., 2010). Furthermore, statistical analyses have been applied to quantify the individual contributions of uncertainty sources as well as the uncertainty arising from their interactions. Several studies have sought to quantify and decompose uncertainties based on their sources. For example, Mujumdar and Ghosh (2008) analyzed streamflow projections and expressed uncertainties from multiple GCMs and emission scenarios in terms of probability distributions using a fuzzy logic-based approach. Hawkins and Sutton (2009, 2011) revealed that time-dependent polynomial trend models can be employed to quantitatively assess sources of uncertainty in precipitation and temperature projections. A similar methodology was also adopted by Orlowsky and Seneviratne (2013), in which fitting a 4th-degree polynomial to drought indices derived from projected meteorological data was made. However, Yip et al. (2011) specifically pointed out that interpreting both total uncertainty and the uncertainty arising from source interactions is not practical with such polynomial approaches. Instead, they demonstrated that variance decomposition analysis (ANOVA) provides a more consistent and interpretable means of partitioning uncertainty sources, particularly variances related to interaction terms. Similar ANOVA-based applications were also carried out by Bosshard et al. (2013) and Vetter et al. (2015), who decomposed uncertainties in projected streamflow characteristics resulting from the use of different GCMs, hydrological models (HMs), bias correction algorithms, and so on.

Just as uncertainties stemming from GCM data, emission scenarios, and other components of climate projections are reflected in primary variables of the hydrological cycle such as precipitation, potential evapotranspiration (PET), and runoff, these uncertainties will inevitably be transmitted to reservoir operation outputs. Therefore, identifying the sources of uncertainty in projections used to assess the future behavior of reservoirs and to forecast reservoir releases will provide critical insights to mitigate potential future risks. While the uncertainty theme has frequently been explored at the macro scale, with emphasis on the hydrological regime in the studies cited above, it is also necessary to unravel how the various factors constituting the modeling chain contribute to reservoir operations and water supply systems.

To address the critical issue highlighted above, this study first generated long-term (2021–2099) meteorological projections for the Tahtali dam reservoir in western Türkiye utilizing multiple RCP scenarios, GCMs, and downscaling methods. Thereafter, inflow projections for the same horizon were produced using seven calibrated HMs driven by the projected meteorological data. Accordingly, the effects of the modeling chain followed, shaped by four main factors, on the operation and optimization of the reservoir releases were investigated. The quantitative contributions of distinct uncertainty sources affecting the modeling process were assessed through a four-way ANOVA approach. All these analyses were conducted on the outputs of a hedging rule integrated into the

parameterization-simulation-optimization framework for the reservoir and were compared with those obtained under the standard operating policy (SOP). The remainder of this paper is structured as follows: Section 2 introduces the data employed in the study, Section 3 describes the methodology applied, Section 4 presents the results and discussion, and the final section draws concluding remarks.

## 2 DATA USED

### 2.1 Study region and observed data

The case study was carried out in the Tahtali watershed ( $554 \text{ km}^2$ ) located in the Küçük Menderes River Basin in western Türkiye. The Tahtali Reservoir, with an active storage capacity of about  $291 \text{ Mm}^3$ , plays an important role in supplying nearly  $128 \text{ Mm}^3/\text{year}$  of fresh water to Izmir city. Given recent shifts in the hydrological regime for this region, reliable reservoir operation has become more essential for sustainable water resources management. For hydrological modeling, naturalized streamflow data from 1970–1988 (prior to dam construction) were used, along with reservoir characteristics and storage-area relations obtained from the State Hydraulic Works of Türkiye. During this observation period, the region received an average annual precipitation of 825 mm and had a mean temperature of  $16^\circ\text{C}$ , while annual runoff was around 285 mm, which is nearly one-third of the precipitation (Ersoy et al., 2025a).

### 2.2 Regional climate simulation

To project future hydro-climatic changes in the Tahtali watershed, data from five GCMs under two RCP scenarios (4.5 and 8.5) were utilized in both dynamically and statistically downscaled forms. Together with seven lumped HMs, the modeling chain produced 140 inflow projection combinations, which also served as required inputs for the reservoir operation analyses (Ersoy et al., 2025b).

Dynamically downscaled climate data for the baseline historical scenario period (1981–2005) and four future horizons (2021–2039, 2040–2059, 2060–2079, 2080–2099) were compiled from the CORDEX database for the Middle East and North Africa (MENA) domain. Outputs from five GCMs (CNRM-CM5, GFDL-ESM2M, EC-EARTH, HadGEM2-ES, and MPI-ESM-MR) were available under both RCP4.5 and RCP8.5. Systematic biases were also corrected using the quantile delta mapping algorithm, which has been shown to preserve relative changes more effectively than other standard methods. According to bias-corrected CORDEX data, projected precipitation changes under RCP4.5 scenario remained generally insignificant throughout most of the century, whereas under RCP8.5 some GCMs indicated notable reductions during specific periods. In contrast, all CORDEX projections consistently reflected warming trends during 2040–2099, with anomalies ranging between  $1.0\text{--}3.0^\circ\text{C}$  under RCP4.5 and  $3.2\text{--}6.0^\circ\text{C}$  under RCP8.5 toward the late century. Besides, HadGEM2-ES in particular projected the strongest warming, consistent with previous findings over the MENA domain (Ozturk et al., 2018).

Moreover, statistical downscaling was conducted via radial basis function networks (RBFNs), which established transfer functions between ERA5 reanalysis predictors and local observations. Predictor selection was carried out using the least absolute shrinkage and selection operator (LASSO) method, and the trained RBFNs with those predictors yielded satisfactory performance, where the Nash–Sutcliffe efficiency (NSE) values exceeded 0.75. After operating RBFNs-based structure, biases in the statistically downscaled data were again corrected with the QDM, as applied to the CORDEX datasets. Results revealed that projected precipitation anomalies from the statistical approach were generally consistent with CORDEX outputs, with only minor deviations. Temperature projections also reflected the overall warming trend, though under RCP8.5 the GFDL-ESM2M and HadGEM2-ES variants pertaining to statistical downscaling application produced anomalies about  $1.0^\circ\text{C}$  lower than their dynamical counterparts. This is possibly due to the parameterization choices in regional climate models, as previously underlined by Thomas et al. (2021).

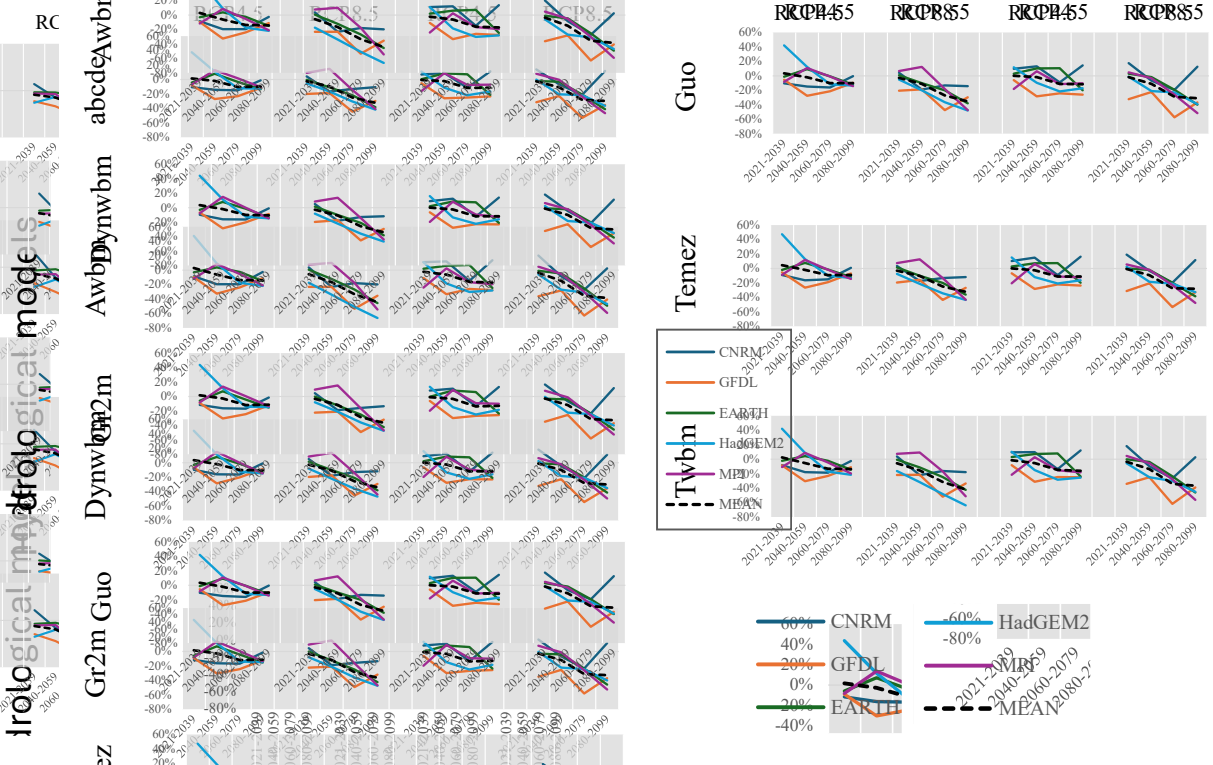


**Figure 1.** Projected changes in annual mean runoff across four future periods under two RCP scenarios. The sub-plots show anomaly projections from five GCMs driven by seven lumped HMs.

### 2.3 Projected runoff data

The hydrological ensemble data were derived from seven lumped HMs (abcde, Awbm, Dynwbm, Gr2m, Guo, Témez, and Twbm), which were previously calibrated under different global optimization algorithms for the Tahtali watershed and validated by Ersoy et al. (2025a). These HMs, which need monthly total precipitation and empirically derived potential evaporation as inputs, achieved NSE values above 0.80 during calibration/validation period and demonstrated their ability to capture overall rainfall–runoff dynamics. However, some HMs (Dynwbm, Gr2m, Guo) showed weaker skill for low flows, as indicated by LNSE values from log-transformed flows, while Twbm performed slightly better in generating both the overall hydrograph and low flow conditions.

In the study, an ensemble of 140 runoff projections was analyzed by comparing twenty-year mean runoff changes ( $\Delta Q$ ) relative to the historical scenario baseline (Figure 1). Accordingly, even marginal precipitation reductions were found to have a considerable impact on  $\Delta Q$ , whereas more severe precipitation decreases under RCP8.5, particularly from GFDL-ESM2M, led to runoff reductions ranging between 27% and 63% after 2060. Also, this GCM accounted for the largest share of statistically significant decreases. On the other hand, MPI-ESM-MR and CNRM-CM5 produced fewer significant variants. Moreover, as for HMs employed, Awbm and Twbm exhibited the most pronounced decreasing runoff trends, while the Guo model showed weaker sensitivity to changing climate inputs. All these findings underscore the strong dependence of runoff projections on how multi-GCM combinations are made and which emission scenarios and HMs they interact with, as previously raised by Wang et al. (2020) and Okkan et al. (2023).

### 3 METHOD

In this study, runoff projections generated by the calibrated HMs were transformed into reservoir inflows and then employed as inputs to reservoir operation optimization modeling (Figure 2). We also used the standard operating policy (SOP), which releases water to fully meet current demand without considering future shortages, for comparison. The employed reservoir operation optimization model in Figure 2 is a nonlinear hedging policy, denoted as HDG-2d, which links monthly release decisions to the corresponding storage levels through a two-dimensional parametric rule. Unlike SOP, this HDG-2d model applies controlled restrictions on reservoir releases so as to minimize the likelihood of severe supply deficits during drought periods (Celeste and Billib, 2009; Okkan et al., 2023).

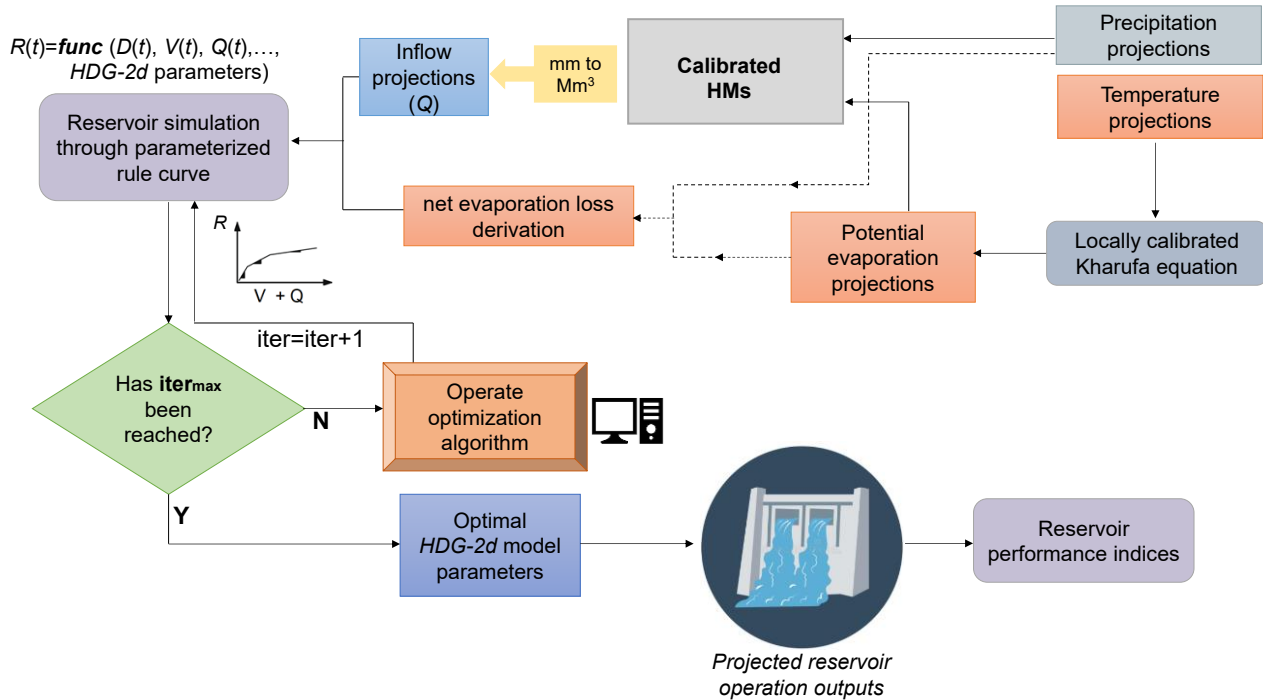


**Figure 2.** Conceptual illustration of the HDG-2d model integrated into the modeling chain framework of this study, adapted from Okkan et al. (2023).

When employing HDG-2d, the objective is to allocate releases that meet demands  $D(t)$  by minimizing the conventional sum of squared deficits. In the mass balance, the release  $R(t)$  is controlled by hedging parameters and net evaporation volume  $E(t)$  is derived iteratively from the area–storage curve, with all variables in  $\text{Mm}^3$ . The related operation rule apply hedging rules through  $hdg(\tau)$ , defined by the combined value (COMV) of active storage and inflow at month  $t$ , i.e.,  $Q(t)$ , as given in Eq. (1).

$$R(t) = \begin{cases} 0, & \text{if } V(t+1) \leq V_{min} \\ D(t) \times \left( \frac{COMV(t)}{hdg(\tau)} \right)^{s(\tau)}, & \text{if } COMV(t) \leq hdg(\tau) \\ D(t), & \text{if } COMV(t) > hdg(\tau) \text{ or } V(t+1) \geq V_{max} \end{cases} \quad (1)$$

where the variable  $COMV(t) = \sqrt{[V(t) - V_{min} - E(t)]^2 + Q(t)^2}$ ;  $s(\tau)$  is the parameter shaping the nonlinearity of the hedging function;  $V(t)$  and  $V(t+1)$  represent the reservoir storage volumes at the beginning and the end of month  $t$ ;  $V_{min}$  and  $V_{max}$  correspond to the reservoir dead volume and maximal storage volume, respectively.

The HDG-2d model has two sets of monthly parameters,  $hdg(\tau)$  and  $s(\tau)$ , for  $\tau = 1, 2, \dots, 12$ , yielding 24 parameters to be calibrated. The shape parameter is restricted to the interval  $[0, 1]$ , while hedging threshold parameter must remain positive and cannot exceed the active reservoir storage for any month  $t$  (Celeste and Billib, 2009).

According to Figure 1, the optimization of the HDG-2d model starts by evaluating the objective function with an initial set of hedging parameters. These parameters were iteratively adjusted by using a differential evolution algorithm coupled with a modified mutation strategy. This adopted framework follows Okkan et al. (2023) without any alteration in the algorithm settings. In total, 140 inflow projections together with projected net evaporation data were considered while calibrating the HDG-2d, and satisfactory convergence was achieved with a population size of 50 and a maximum iteration number ( $iter_{max}$ ) of 300. After model calibration under various conditions, the long-term performance of the case reservoir was assessed using the dimensionless vulnerability index (VUL). This index was preferred because it quantifies the expected value of supply deficits and follows the formulation of Sandoval-Solis et al. (2011).

## 4 RESULTS AND DISCUSSION

The results are based on the evaluation of reservoir operation models under multiple inflow projections. A uniform monthly demand of  $10.667 \text{ Mm}^3$  ( $128 \text{ Mm}^3/\text{year}$ ) was defined for the Tahtali Reservoir, since higher or increasing demands produced unrealistic regulation ratios relative to its planning conditions. While SOP required no iterative procedure excluding net evaporation loss estimation, the nonlinear HDG-2d framework was optimized with DEA, executed 10 times per variant with a stopping criterion of 300 iterations, as described in the previous section. Table 1 outlines the behavioral contrasts between SOP and HDG-2d, based on statistics from an ensemble of 140 reservoir operation projections. This table verifies that the SOP resulted in a higher frequency of severe single-period shortages as drought intensity became more apparent.

**Table 1.** Comparative statistics of reservoir performance indices under SOP and HDG-2d, derived from 140 projection variants.

Performance indices	Models	Mean	Median	Minimum	Maximum
Volume-based reliability	HDG-2d	0.875	0.887	0.605	1
	SOP	0.907	0.922	0.652	1
Dimensionless vulnerability index	HDG-2d	0.177	0.179	0	0.403
	SOP	0.772	0.795	0	0.907

The experiments pointed out that the HDG-2d model is generally characterized by relatively higher  $hdg$  values and lower shape parameters for wetter months. This process also allowed for allocating partial reservoir releases during drier periods. Because of the large number of simulations, they are not presented here. These calibrated parameters were observed to gradually restrict releases in the early stages of the projection horizon. Of course, this hedging application bring about a slight decrease in volume-based reliability indices (Table 1). The parametrization of HDG-2d reflects a system behavior aimed at preparing the reservoir for severe drought conditions and kept VUL values at approximately one-fourth of the values obtained under the SOP, as seen in Table 1.

The variability of projected VUL values across different sources of uncertainty was visualized by using box plots (Figure 3). For each uncertainty source, these plots were generated by combining the other remaining components of the modeling chain. For instance, the figure presents HM-specific findings showing VUL distributions from 20 projection variants ( $5 \text{ GCMs} \times 2 \text{ ESs} \times 2 \text{ DMs}$ ), while GCM-specific ones were collected from 28 projection combinations. Figure 3 also demonstrates that HDG-2d substantially reduces the severe vulnerabilities observed under SOP, independent of the uncertainty source. Another observation is that under SOP, selection of HM strongly influences VUL outcomes, as seen in the notable median shifts among reservoir operation models.

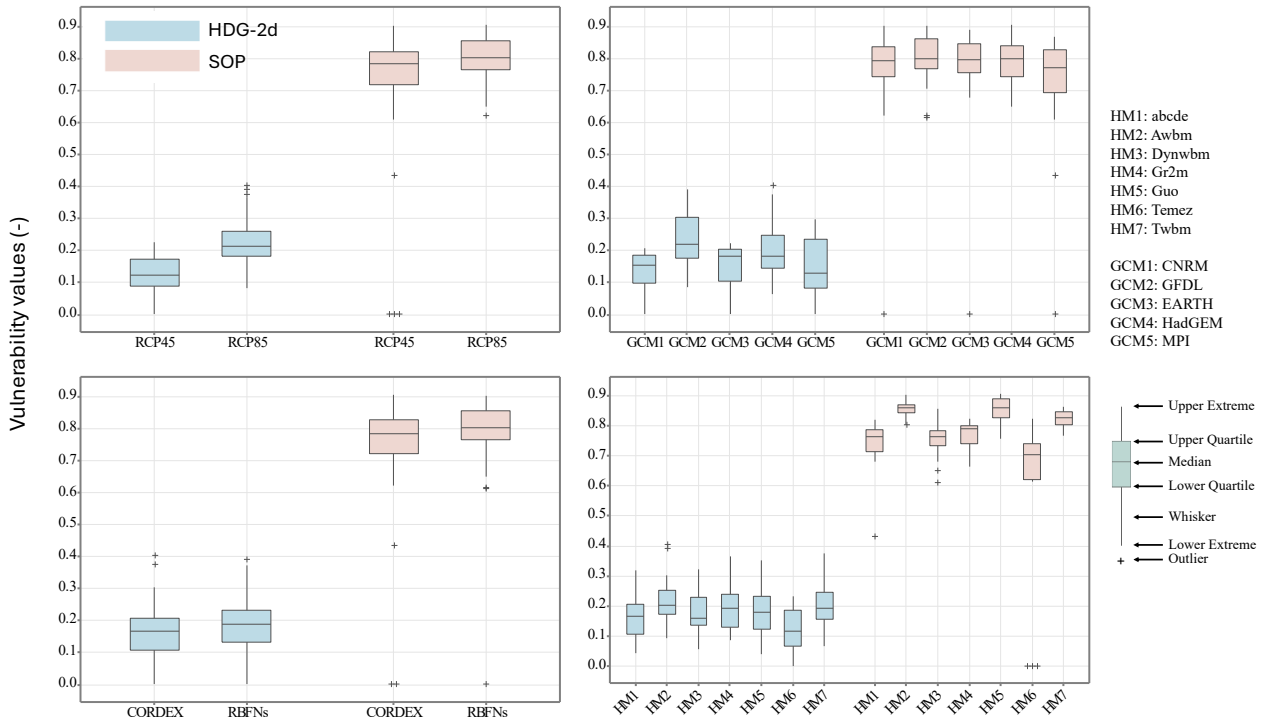


**Figure 3.** Projected vulnerability values (VUL) under two reservoir operation models, stratified by four key uncertainty factors. Each panel represents the distribution of vulnerability values related to a single factor: RCP scenarios (top-left), GCMs (top-right), downscaling data types (bottom-left), and HMs (bottom-right)

The system vulnerability projections were also examined by the four-way ANOVA approach, of which procedure is outlined by Vetter et al. (2015). It is obvious from Figure 4 that the HM selection accounted for 36% of the total variance for projected VUL values (Ersoy et al., 2025b). Moreover, nonlinear interactions between HMs and other uncertainty sources contributed even more to the overall interaction variance under SOP. Interestingly, HDG-2d model meaningfully tempered HM-induced variances for that performance measure and thus diminished the overall uncertainty compared to that of SOP (Figure 4).

Although projected annual mean streamflow changes under the HIST scenario suggest that HM-related uncertainty is limited (not shown), the applied HMs differ in their ability to represent fundamental hydrological processes. Consequently, runoff simulated by these monthly HMs under different climate conditions can vary both in magnitude and in interannual fluctuations. In particular, LNSE outcomes indicate that certain HMs have difficulty in reproducing low-flow regimes (Ersoy et al., 2025a), and discrepancies are also detected across models in terms of baseflow indices and low-flow durations. The simple rule of a model such as SOP cannot adapt to these inconsistencies, instead allocating inflows directly to meet target demands. This lack of adaptability often reduces the sustainability of releases, producing higher and more uncertain VUL values, as seen in Figure 3 and 4. As HM selection uncertainty has a stronger influence on low-flow projections than on annual means (Wang et al., 2020), SOP is ineffective at dampening this HM-related low-flow variability, thereby amplifying overall uncertainty. By contrast, the HDG-2d model can regulate releases in advance through its parametric rule structure, even under low-flow conditions. According to Ersoy et al. (2025b), this could be achieved by its buffering capacity preventing inflow disparities induced by employed HMs from directly propagating to projected VUL values.

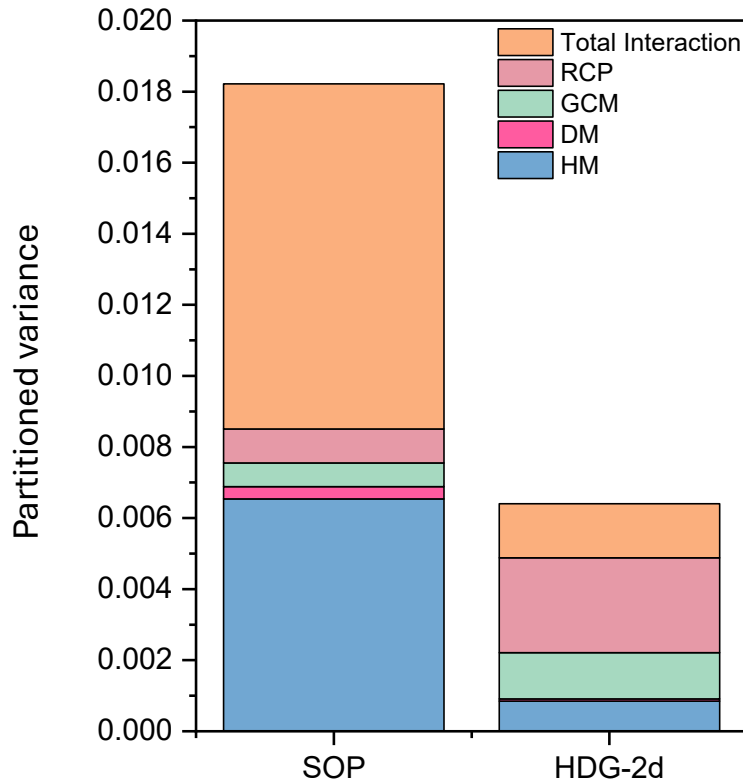


**Figure 4.** Portioned variances for projected VUL values, attributed to key uncertainty sources, together with their combined interaction.

Even though HDG-2d reduced overall uncertainty with regard to VUL by 65% through reducing the huge variances from HMs and their interactions, GCMs and RCPs still accounted for two-thirds of the total variance, showing the model's sensitivity to climate-related signals (Figure 4). Since HDG-2d prioritizes moderating flow deficits, GCM and scenario effects can become more prominent when this adaptive model incorporates changing climate signals into release decisions. Unlike SOP, this led to a reversed pattern, where distinct climate forcings cause relatively greater spread in hedging responses and VUL values. This is likely because the HDG-2d model exhibited higher sensitivity to some drying GCMs such as GFDL-ESM2M, with the GCM-related share of variance roughly doubling compared to that of SOP.

It should be emphasized that HDG-2d adjusts its hedging strategy separately for each RCP, with its parameters being more strongly shaped by emission scenario selected than by differences among GCMs. The first panel of Figure 4 illustrates an indication of how scenario-related uncertainty compares in relative importance. Under RCP8.5, marked by strong radiative forcing, HDG-2d generally imposes stricter release restrictions, which broadens the ensemble interquartile range and highlights emission scenario-based uncertainty for vulnerability (Figure 4). Since RCP choice is increasingly influential on projected temperature and evaporation trends rather than annual mean runoff (Ersoy et al., 2025b), the stronger RCP uncertainty under HDG-2d suggests that its calibration effectively responds to these changing climate signals. Therefore, achieving low scenario uncertainties under the SOP, which cannot suppress HM-based disparities under low-flow conditions and is not sensitive to emission-induced shifts because of its simplicity, cannot be considered a mark of robustness when accompanied by the higher VUL values it produced.

## 5 CONCLUSIONS

Reservoirs that were originally designed under stationary hydrological records now experience increased vulnerability, with uncertainty propagating under climate change–driven alterations in reservoir inflows. This study assessed reservoir operation performance under climate

change uncertainty for an example reservoir operated in the western part of Türkiye by comparing the traditional SOP model and the adaptive HDG-2d model across 140 projected vulnerability values. The findings showed that SOP amplified hydrological model–driven volatility and produced higher vulnerability levels, while HDG-2d reduced total uncertainty by more than 50% and ensured that most projections remained below critical vulnerability thresholds. Moreover HDG-2d maintained responsiveness to climate forcing derived from multiple GCMs and emission scenarios. This demonstrates that the framework applied not only buffers modeling discrepancies but also effectively incorporates external climate signals into reservoir releases. Overall, we also highlight that adaptive hedging modeling can provide more robust and uncertainty-aware reservoir operation strategies, while irreducible GCM and scenario uncertainties as well as internal variabilities remain a key challenge for credible water resources planning. Furthermore, more detailed analyses on this topic, including alternative crop patterns for irrigation purposes, are being addressed in a separate ongoing study.

## ACKNOWLEDGEMENTS

This study is funded by the Scientific and Technological Research Council of Türkiye (TÜBİTAK) under Grant No. 122Y083. The authors gratefully acknowledge the support provided by TÜBİTAK during the course of this research.

## REFERENCES

Bosshard, T., Carambia, M., Goergen, K., Kotlarski, S., Krahe, P., Zappa, M., Schär, C. (2013). Quantifying uncertainty sources in an ensemble of hydrological climate-impact projections. *Water Resources Research*, 49(3), 1523–1536. <https://doi.org/10.1029/2011WR011533>

Bozkurt, D., Sen, O. L., Hagemann, S. (2015). Projected river discharge in the Euphrates-Tigris Basin from a hydrological discharge model forced with RCM and GCM outputs. *Climate Research*, 62(2), 131-147. <https://doi.org/10.3354/cr01268>

Celeste, A. B., and Billib, M. (2009). Evaluation of stochastic reservoir operation optimization models. *Advances in Water Resources*, 32(9), 1429-1443. <https://doi.org/10.1016/j.advwatres.2009.06.008>

Ersoy, Z. B., Fistikoglu, O., Okkan, U., Derin, B. (2025a). Convergence and final performances of optimization algorithms for rainfall-runoff model calibration based on the number of function calls. *Earth Science Informatics*, 18(2), 382. <https://doi.org/10.1007/s12145-025-01885-y>

Ersoy, Z. B., Fistikoglu, O., Okkan, U. (2025b). Uncertainty-Aware Reservoir Operation Projections Using Multi-Model Weighting and Adaptive Hedging Rules. *Journal of Hydrology*, under review.

Hawkins, E., and Sutton, R. (2009). The potential to narrow uncertainty in regional climate predictions, *Bulletin of the American Meteorological Society*, 90(8), 1095-1108. <https://doi.org/10.1175/2009BAMS2607.1>

Hawkins, E., and Sutton, R. (2011). The potential to narrow uncertainty in projections of regional precipitation change, *Climate Dynamics*, 37(1-2), 407–418. <https://doi.org/10.1007/s00382-010-0810-6>

Knutti, R., Sedláček, J., Sanderson, B. M., Lorenz, R., Fischer, E. M., Eyring, V. (2017). A climate model projection weighting scheme accounting for performance and interdependence. *Geophysical Research Letters*, 44(4), 1909-1918. <https://doi.org/10.1002/2016GL072012>

Mujumdar, P. P., and Ghosh, S. (2008). Modeling GCM and scenario uncertainty using a possibilistic approach: Application to the Mahanadi River, India. *Water Resources Research*, 44(6). <https://doi.org/10.1029/2007WR006137>

Okkan, U., Fistikoglu, O., Ersoy, Z. B., Noori, A. T. (2023). Investigating adaptive hedging policies for reservoir operation under climate change impacts. *Journal of Hydrology*, 619, 129286. <https://doi.org/10.1016/j.jhydrol.2023.129286>

Okkan, U., Fistikoglu, O., Ersoy, Z. B., Noori, A. T. (2024). Analyzing the uncertainty of potential evapotranspiration models in drought projections derived for a semi-arid watershed. *Theoretical and Applied Climatology*, 155(3), 2329-2346. <https://doi.org/10.1007/s00704-023-04817-2>

Orlowsky, B., and Seneviratne, S. I. (2013). Elusive drought: uncertainty in observed trends and short-and long-term CMIP5 projections. *Hydrology and Earth System Sciences*, 17(5), 1765-1781. <http://doi.org/10.5194/hess-17-1765-2013>

Ozturk, T., Turp, M. T., Türkeş, M., Kurnaz, M. L. (2018). Future projections of temperature and precipitation climatology for CORDEX-MENA domain using RegCM4.4, *Atmospheric Research*, 206, 87-107. <https://doi.org/10.1016/j.atmosres.2018.02.009>

Sandoval-Solis, S., McKinney, D. C., Loucks, D. P. (2011). Sustainability index for water resources planning and management. *Journal of Water Resources Planning and Management*, 137(5), 381-390. [https://doi.org/10.1061/\(ASCE\)WR.1943-5452.0000134](https://doi.org/10.1061/(ASCE)WR.1943-5452.0000134)

Thomas, T., Ghosh, N. C., Sudheer, K. P. (2021). Optimal reservoir operation—A climate change adaptation strategy for Narmada basin in central India. *Journal of Hydrology*, 598, 126238. <https://doi.org/10.1016/j.jhydrol.2021.126238>

Vetter, T., Huang, S., Aich, V., Yang, T., Wang, X., Krysanova, V., Hattermann, F. (2015). Multi-model climate impact assessment and intercomparison for three large-scale river basins on three continents. *Earth System Dynamics*, 6(1), 17-43. <https://doi.org/10.5194/esd-6-17-2015>

Wang, H. M., Chen, J., Xu, C. Y., Zhang, J., Chen, H. (2020). A framework to quantify the uncertainty contribution of GCMs over multiple sources in hydrological impacts of climate change. *Earth's Future*, 8(8), e2020EF001602. <https://doi.org/10.1029/2020EF001602>

Yip, S., Ferro, C. A., Stephenson, D. B., Hawkins, E. (2011). A simple, coherent framework for partitioning uncertainty in climate predictions. *Journal of Climate*, 24(17), 4634-4643. <https://doi.org/10.1175/2011JCLI4085.1>